**CONFERENCE PRE-PRINT**

# BREAKTHROUGH IN PERFORMANCE DEGRADATION OF ITER CENTRAL SOLENOID CONDUCTORS OWING TO SHORT-TWIST-PITCH CABLING AND SUPPRESSION OF BENDING STRAIN

Tomone SUWA, Takaaki ISONO, Keiya TAKEBAYASHI, Yasuhiro UNO, Tsutomu KAWASAKI, Masaru. KAWABE and Tsutomu HEMMI
National Institutes for Quantum Science and Technology
Mukoyama 801-1, Naka, Japan
Email: suwa.tomone@qst.go.jp

**Abstract**

In developing the ITER central solenoid (CS) conductors, performance degradation due to electromagnetic loading cycles was identified as a critical issue. This issue was addressed by developing conductors having a short twist pitch, resulting in stable $T_{cs}$ under electromagnetic loading cycles. While this degradation issue has been resolved, the contribution of the strain state of the $Nb_3Sn$ strands within the conductor to its performance remains unclear, and the mechanism by which the short twist pitch mitigates $T_{cs}$ degradation has not yet been clarified. To support the development of future conductors for DEMO, strain analysis based on previous test results was performed to investigate both the mechanism by which the short twist pitch mitigates performance degradation and the strain state under actual operating conditions.

## 1. INTRODUCTION

The ITER central solenoid (CS) is a large-scale superconducting coil, 13-meters high and 4-meters wide, which allows a large current to be induced in the plasma. The CS conductors are cable-in-conduit conductors, 918 m (613 m) in unit length for a hexa-pancake (quadri-pancake) coil and are composed of a superconducting cable and JK2LB stainless steel jackets, as shown in Fig. 1. The superconducting cable is composed of a five-stage cable having 576 $Nb_3Sn$ and 288 Cu strands and a central spiral. At the start of discharge (SOD), the CS will be operated under a peak magnetic field of 13 T, generated by a 40-kA current flowing at 4 K. Therefore, the CS conductors are expected to be subjected to 60,000 electromagnetic loading cycles owing to the high current and magnetic field in 30,000 plasma burns over the lifetime of ITER [1].

As illustrated in Fig. 1, strain is induced in the $Nb_3Sn$ strands by compressive thermal stress due to the variation of thermal contraction between the jacket and the cable, and by electromagnetic loading during energization. In this case, the electromagnetic force is a combination of the Lorentz force and the compressive force exerted by adjacent strands. During CS operation, hoop stress is also applied to the conductor. Because the critical current ($I_c$) of the $Nb_3Sn$ strands also degrades due to the strain, conductor performance also degrades due to these forces. During the development of the CS conductors, performance degradation caused by electromagnetic loading cycles was a major concern. This issue was resolved by developing short-twist-pitch conductors having increased stiffness. However, the strain dependence of conductor performance has not yet been fully clarified. To support the development of future conductors for DEMO, the strain state within the short-twist-pitch conductors and under actual operating conditions was analysed based on previous test results.

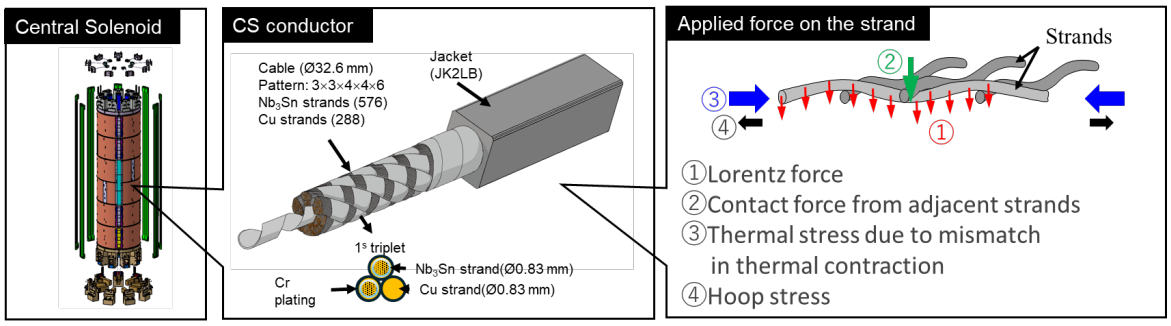


*Fig. 1 ITER central solenoid (CS) and schematic of forces applied on the $Nb_3Sn$ strands in the CS conductor during operation.*

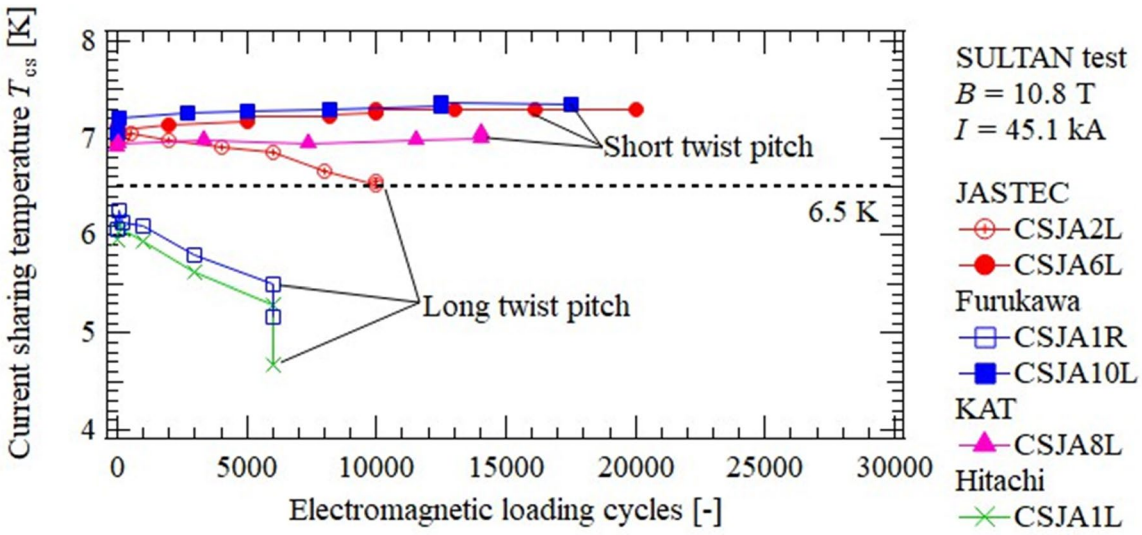


*Fig. 2 Current sharing temperature ($T_{cs}$) of representative CS conductors after electromagnetic loading cycles*

TABLE 1 COMPARISON OF CS CONDUCTORS

| item | | Long twist pitch | Short twist pitch |
|---|---|---|---|
| Cable Pattern | | $(2Nb_3Sn + 1Cu) \times 3 \times 4 \times 4 \times 6$ | |
| Twist pitch [mm] | 1st | 45±5 | 20±5 |
| | 2nd | 85±10 | 45±5 |
| | 3rd | 125±10 or 145±10 | 80±10 |
| | 4th | 250±15 | 150±15 |
| | 5th | 450±20 | 450±20 |
| Jacket material | | JK2LB | JK2LB |
| Inner diameter [mm] | | 32.6 | 32.6 |
| Outer dimension [mm] | | 49.0 × 49.0 | 49.0 × 49.0 |
| Void fraction [%] | | 33.4 | 32.4 |

## 2. CS CONDUCTOR DEGRADATION

To evaluate the performance of CS conductors under approximately 10,000 electromagnetic loading cycles, the current sharing temperature ($T_{cs}$) of several 3.6-m, straight samples was measured at the SULTAN facility [2]. Since the maximum background field of the SULTAN facility is lower than 13 T, the test conditions were selected to reproduce the maximum electromagnetic loading in the ITER CS by using a background field of 10.85 T and current of 45.1 kA. In the early phases of CS conductor development, several prototype conductors having long twist pitch cables were manufactured as the baseline, the main specifications of which are shown in Table 1. However, the $T_{cs}$ of those conductors degraded after less than 10,000 cycles, as shown in Fig. 2 [3]. Visual inspections of the CS conductors whose $T_{cs}$ degraded revealed bent and buckled strands, as shown in Fig. 3. Moreover, large, local bending of the $Nb_3Sn$ strands in the conductors was identified by neutron diffraction measurements, which raised concerns that the long-twist-pitch conductors were not appropriate for the CS.

## 3. IMPROVEMENT BY SHORTENING TWIST PITCH

In general, the critical buckling load is inversely proportional to the support length, and deflection of the strands exhibits a polynomial dependence on the support length. Since the twist pitch corresponds to the support length, it was considered that a short twist pitch can mitigate $T_{cs}$ degradation caused by strand deformation due to electromagnetic loading. Therefore, short-twist-pitch conductors were developed by reducing the twist pitch to nearly half that of the long-twist-pitch conductors, as shown in Table 1, with the exception of the 5th stage cable. Fig. 4 shows the surfaces of the 5th stage cables. Using the newly developed short-twist-pitch CS conductors, $T_{cs}$ no longer degraded due to electromagnetic loading cycles, but $T_{cs}$ increased by several percent, as shown in Fig. 2.

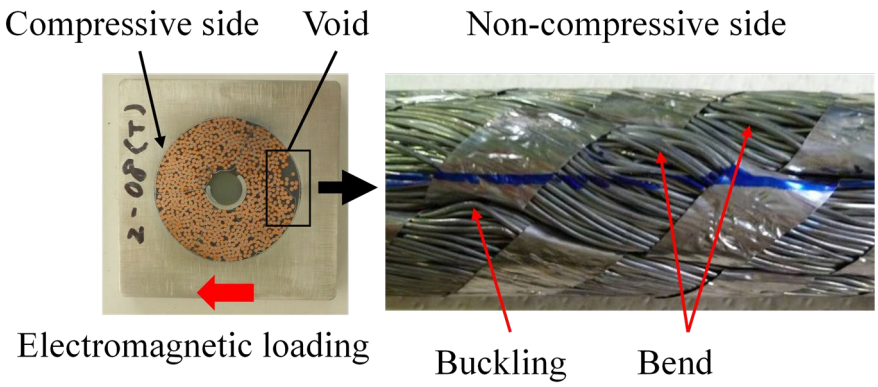


*Fig. 4 Visual inspections of the long twist pitch CS conductor whose $T_{cs}$ degraded*

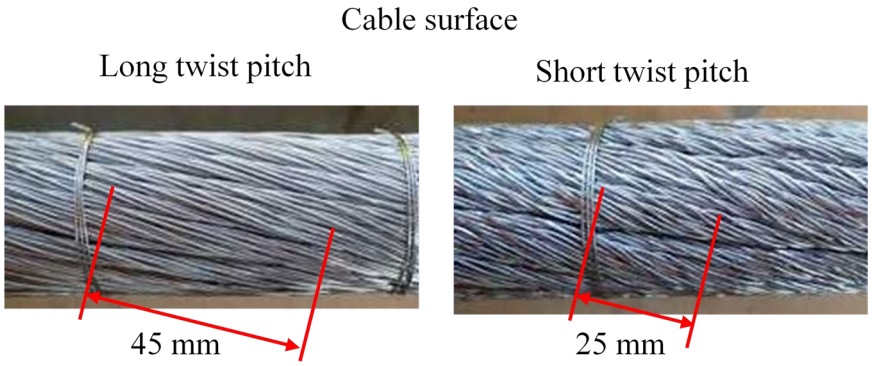


*Fig. 4 Surfaces of the 5th stage cable for the long and short twist pitch conductors.*

## 4. ANALYSIS OF STRAIN INDUCED BY ELECTROMAGNETIC LOADING IN SULTAN TEST RESULTS

To investigate the influence of strain induced by electromagnetic forces during energization on conductor performance, an evaluation using effective strain was performed [4]. Effective strain $\varepsilon_{eff}$ was defined as an equivalent axial strain that characterizes the $T_{cs}$ in the SULTAN caused by compressive thermal strain and strain induced by electromagnetic loading $F_{EM}$. It was assumed in the evaluation that effective strain is uniformly applied to the $Nb_3Sn$ strands in a uniaxial direction along the conductor. Under this assumption, the electric field–temperature curve was determined by the following equation:

$$E = \frac{E_c}{L_V A} \int \int \left( \frac{I_{op}/N_{SC}}{I_c(B, T, \varepsilon_{eff})} \right)^n dAdz \quad (1)$$

where, $E_c$ is 10 μV/m, $L_v$ is the voltage tap length, $A$ is cross-sectional area of the cable, $I_{op}$ is operating current, $N_{sc}$ is the number of $Nb_3Sn$ strands, and $n$ is n-value. $I_c$ is the critical current of $Nb_3Sn$ strands as a function of magnetic field $B$, temperature $T$, and strain. $F_{EM}$ was calculated by multiplying the operating current and the magnetic field.

Fig. 5 shows the $\varepsilon_{eff}$ vs $F_{EM}$ plot of long-twist-pitch and short-twist-pitch conductors after electromagnetic loading cycles. The lines show linear fitting results. If strain in the $Nb_3Sn$ strands within the conductor is induced by electromagnetic loading, the gradient of the $\varepsilon_{eff}$ vs $F_{EM}$ plot is expected to become large. In the case of long-twist-pitch conductors, the $Nb_3Sn$ strands may be easily bent by electromagnetic loading, which is considered to result in a large gradient ($-5.2\times10^{-4}$%kN$^{-1}$m$^{-1}$) in the $\varepsilon_{eff}$ vs $F_{EM}$ plot. On the other hand, a small gradient ($-1.9\times10^{-5}$%kN$^{-1}$m$^{-1}$) was observed in the short-twist-pitch conductor, most likely from the increased cable stiffness owing to the short twist pitch, which reduces bending strain caused by electromagnetic loading. However, this hypothesis (reduction of bending strain by short twist pitch) cannot be validated through effective strain evaluation alone, for

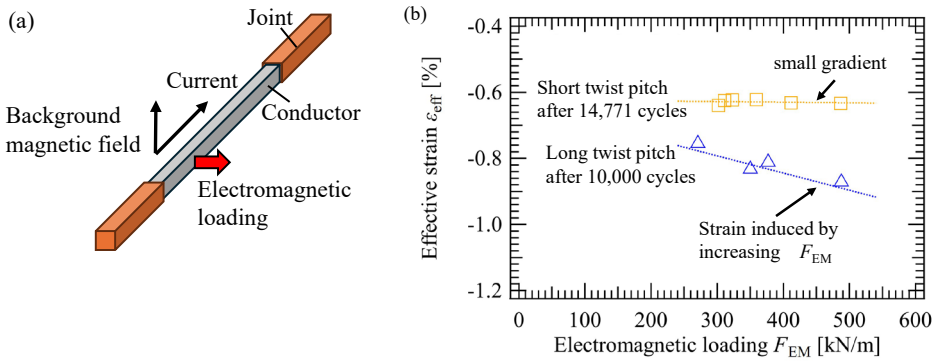


*Fig. 5 (a)Schematic of SULTAN sample. (b) Electromagnetic loading $F_{EM}$ dependence of effective strain $\varepsilon_{eff}$ on the long and the short twist pitch CS conductors after the electromagnetic loading cycles.*

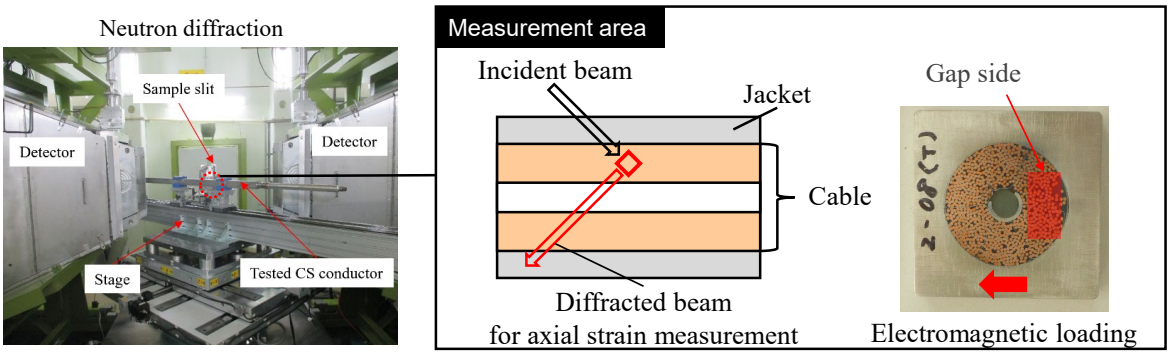


*Fig. 6 Neutron diffraction measurement at J-PARC Takumi.*

the following reasons. First, axial and bending strains cannot be distinguished from effective strain. Second, if the $I_c$ of the $Nb_3Sn$ strands changes due to factors unrelated to strain, this could result in an apparent change in effective strain. Consequently, variation in the $I_c$ of $Nb_3Sn$ strands used in different conductors may be observed as apparent effective strain. Therefore, a comparison of effective strain between long and short twist pitches may reflect not only strain but also other contributing factors.

## 5. INTERNAL STRAIN ANALYSIS BY NEUTRON DIFFRACTION

Since the detailed strain state cannot be evaluated using only effective strain, the residual strain in the $Nb_3Sn$ strands within the conductor was directly measured by neutron diffraction as shown in Fig. 6. If the strain induced by electromagnetic loading is sufficiently large to cause plastic deformation of the $Nb_3Sn$ strands within the conductor, the electromagnetic loading cycles may result in the accumulation of permanent strain and deformation. As a result, $T_{cs}$ is considered to degrade continuously after the electromagnetic loading cycles. Through measurement of the residual strain in the $Nb_3Sn$ strands within the conductor after the SULTAN test, it is possible to assess the extent of the permanent strain induced by the electromagnetic loading cycles.

To investigate whether the mitigation of $T_{cs}$ degradation was caused by the suppression of permanent bending strain owing to the short twist pitch, residual strain measurements at the gap side (shown in Fig. 7) using neutron diffraction were performed on the long and short twist pitch CS conductors after the SULTAN test [5,6]. Because the two conductors were fabricated using $Nb_3Sn$ strands from different suppliers, stress-free samples (extracted $Nb_3Sn$ filaments) from each conductor were also measured and used as reference profiles. The strain distributions in the conductors were calculated by deconvolving the measured profiles of the conductors using the reference profiles. This approach excluded the influence of differences between the two conductors due to the use of $Nb_3Sn$ strands from different suppliers. Figure 7 shows these results. In the SULTAN test, a magnetic field distribution exists along the axial direction of the conductor. In the high-field zone where $T_{cs}$ was measured, the conductor was subjected to electromagnetic loading. On the other hand, the electromagnetic loading was almost zero in the low-field zone where the magnetic field was nearly zero. Accordingly, it was assumed that the strain state in the low-field zone remained unchanged before and after the SULTAN test. In general, a broadened profile was observed when bending strain occurs. Consequently, the variation in strain distribution between the low-field and

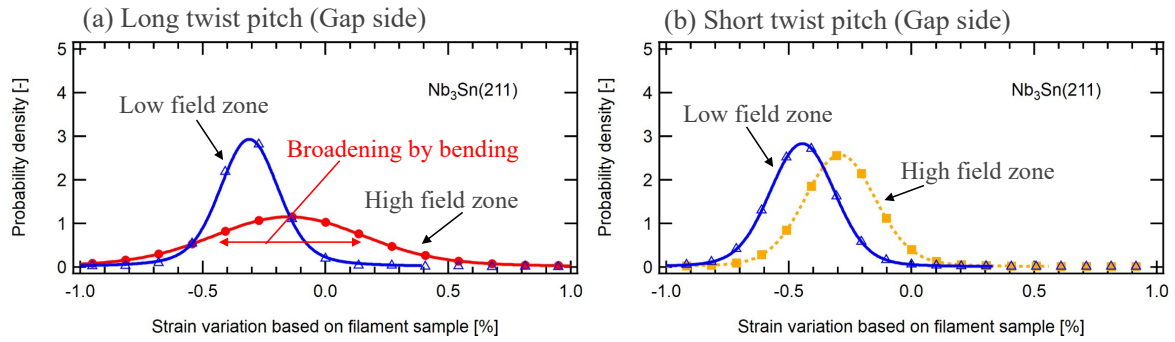


*Fig. 7 Strain distribution of (a) the long and (b) short twist pitch conductors after the electromagnetic loading cycles.*

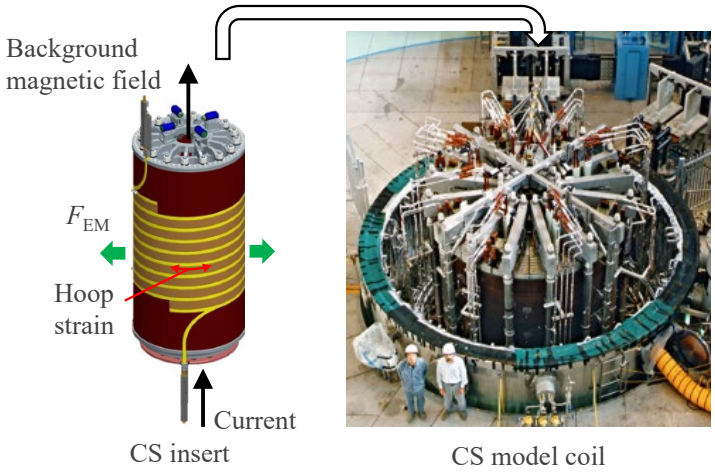


*Fig. 8 Schematic of the CS insert. The CS insert was put in a CS model coil to apply a background magnetic field.*

high-field zones makes it possible to estimate residual bending strain caused by electromagnetic loading cycles. The calculated mean values and variations of residual bending strain caused by the electromagnetic loading cycles were 0.53±0.32% in the long-twist-pitch conductor and 0.10±0.07% in the short-twist-pitch conductor [5]. These findings show that the short twist pitch effectively mitigates permanent bending strain from electromagnetic loading cycles, resulting in the suppression of $T_{cs}$ degradation. Furthermore, relaxation of axial strain (about 0.16%) was observed in both conductors. This result may indicate that the several-percent increase in $T_{cs}$ observed in the short-twist-pitch conductors after electromagnetic loading cycles is due to the relaxation of axial strain.

## 6. INFLUENCE OF HOOP STRAIN

During the actual CS operation, tensile hoop stress and strain are applied to the conductor. It is expected that this tensile strain will reduce the compressive thermal strain in the $Nb_3Sn$ strands within the conductor. However, the hoop strain could not be reproduced in the SULTAN test because straight samples were used. As a result, $T_{cs}$ measured in the SULTAN test was considered to be lower than that in the actual CS operation. To evaluate the impact of hoop strain, both a cylindrical CS insert (Fig. 7 (a)) and a straight sample were fabricated from the same conductor, and the two samples were tested. To reproduce the conditions of actual CS operation, the test of the CS insert was carried out using a CS model coil to apply a background magnetic field. The straight sample was tested in the SULTAN facility. In these tests, a higher $T_{cs}$ was observed in the CS insert (7.7 K) compared to the SULTAN sample (7.3 K) after the electromagnetic loading cycles [7,8].

Since both samples were made from the same conductor, it is assumed that the strain (including bending strain) induced by electromagnetic loading is similar in both the CS insert and the SULTAN sample. Therefore, the difference in the gradient of the $\varepsilon_{eff}$ vs $F_{EM}$ plot is considered to be caused by hoop strain. Fig. 9 shows the $\varepsilon_{eff}$ vs $F_{EM}$ plots. In the case of normal and reverse charging of the CS insert after the electromagnetic loading cycle, the

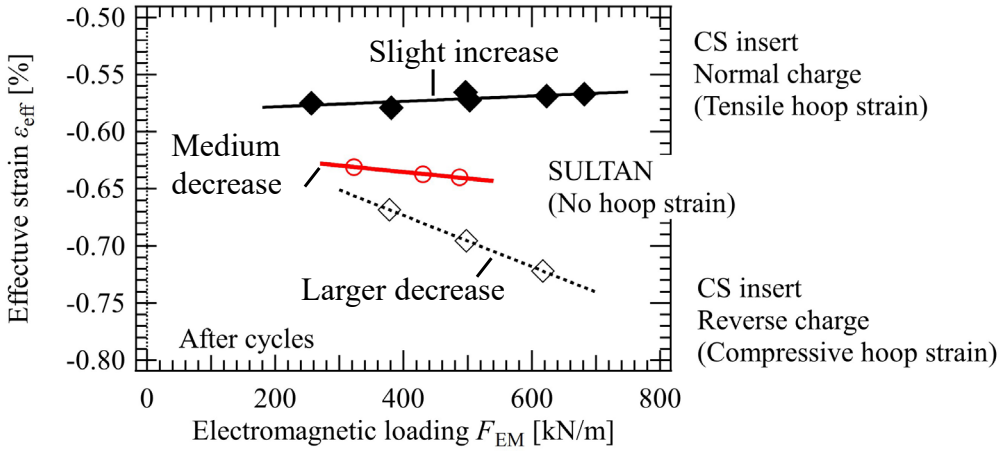


*Fig. 9 Electromagnetic loading $F_{EM}$ dependence of effective strain $\varepsilon_{eff}$ for CS insert and SULTAN sample.*

gradients of $\varepsilon_{eff}$ vs $F_{EM}$ plots were $2.3\times10^{-5}$%kN$^{-1}$m$^{-1}$ and $-22.4\times10^{-5}$%kN$^{-1}$m$^{-1}$, respectively. The gradient of the SULTAN sample was $-5.6\times10^{-5}$%kN$^{-1}$m$^{-1}$ after the electromagnetic loading cycles. The relaxation of thermal compressive strain due to tensile hoop strain is considered to have exceeded the degradation caused by strain induced by electromagnetic loading, resulting in the slight positive gradient for the normal charging of the CS insert. On the other hand, compressive hoop strain is considered to have added to the thermal strain, resulting in the large negative gradient in the reverse charging of the CS insert. Due to no hoop strain in the SULTAN sample, the intermediate gradient between those of the CS insert was observed. Therefore, the higher $T_{cs}$ observed in the CS insert compared to that of the SULTAN sample can be explained by the influence of hoop strain.

## 7. ADVANTAGE OF SHORT-TWIST-PITCH CONDUCTORS

Based on the results of the SULTAN test, the smaller gradient of the $\varepsilon_{eff}$ vs $F_{EM}$ plots observed in the short-twist-pitch CS conductor may indicate that deformation was almost maintained within the elastic range. As a result, permanent (plastic) strain accumulation of the $Nb_3Sn$ strands during electromagnetic loading cycles was effectively mitigated. As supported by the neutron diffraction measurements, it was confirmed that the anticipated suppression of permanent bending strain by the short twist pitch contributed to the mitigation of $T_{cs}$ degradation. Therefore, these results support that a short-twist-pitch conductor will be appropriate for the future DEMO device to maintain $T_{cs}$ after the electromagnetic loading cycles. Moreover, an increase in $T_{cs}$ is expected during operation due to the relaxation of compressive thermal strain caused by tensile hoop strain, in the case that this effect exceeds the degradation due to strain induced by the electromagnetic loading. Additionally, the small gradient of the $\varepsilon_{eff}$ vs $F_{EM}$ plot may indicate that degradation will be mitigated under higher electromagnetic forces than those in ITER (520 kN/m).

## 8. CONCLUSION

In the ITER CS conductor manufacturing, short-twist-pitch CS conductors were developed to solve the $T_{cs}$ degradation caused by the electromagnetic loading cycles. The results of strain analysis indicated that the suppression of bending strain effectively mitigated $T_{cs}$ degradation. It was also found that hoop strain influences $T_{cs}$. Based on these results, the following insights have been obtained for the future development of conductors for DEMO. The short-twist-pitch design is expected to maintain its performance due to the reduction of the bending strain even under the higher electromagnetic forces in DEMO. Since hoop stress could not be applied to the samples in SULTAN, these results are considered conservative. However, the SULTAN test is effective for qualification. To quantitatively evaluate the influence of hoop stress on conductor performance, testing with a cylindrical sample like the CS insert is necessary. If the correlation between effective strain and actual strain in $Nb_3Sn$ strands is further clarified, future conductors can be developed using effective strain as a benchmark.

## REFERENCES

[1] A. Devred, et al., Status of Conductor Qualification for the ITER Central Solenoid, IEEE Trans. Appl. Supercond. 23, (2013) 6001208.

[2] P. Bruzzone, et. al., Test of ITER conductors in SULTAN: An update, Fus. Eng. Des. **86** (2011) 1406-1409.
[3] T. HEMMI, et al., Test Results and Investigation of Tcs Degradation in Japanese ITER CS Conductor Samples, Supercond. Sci. Technol. **26** (2013) 084002.
[4] D. Bessette, Modeling techniques for correcting measured data on the ITER toroidal field insert coil, IEEE Trans. Appl. Supercond., **14** (2004), 1418–1422.
[5] T. HEMMI, et al., Neutron diffraction measurement of internal strain in the first Japanese ITER CS conductor sample, Supercond. Sci. Technol. 26, (2013) 084002.
[6] T. SUWA, et al., Strain analysis by neutron diffraction on Nb3Sn strands in ITER central solenoid conductors of short and long twist pitch, Supercond. Sci. Technol. 38, (2024) 015008.
[7] Y. NABARA, et al., Current-sharing Temperature Characteristics of ITER Central Solenoid Insert coil, J. Cryo. Super. Soc. Jpm. 51, (2016) 102
[8] N. Martovetsky, et al., ITER Central Solenoid Insert Test Results, IEEE Trans. Appl. Supercond. 26, (2016) 4200606.